

CONFERENCES AND SYMPOSIA

PACS numbers: **75.85.+t**, **85.70.–w**, **85.75.–d**

Micromagnetism and topological defects in magnetoelectric media

A P Pyatakov, A S Sergeev, E P Nikolaeva, T B Kosykh, A V Nikolaev,
K A Zvezdin, A K Zvezdin

DOI: 10.3367/UFNe.0185.201510k.1077

Contents

Abstract. This paper briefly reviews research of the magnetoelectric materials and multiferroics as domain-structured media. The review is focused on magnetoelectric phenomena in epitaxial iron garnet films (electrically induced displacement and tilting of domain boundaries) as a striking example of magnetoelectricity in micromagnetism. The paper also considers the effect of an electric field on other topological defects in magnetically ordered media, including Bloch lines and Bloch points at domain boundaries, magnetic vortices, and skyrmions.

Keywords: multiferroics, magnetoelectric effect, domain wall, skyrmion, Bloch line, Bloch point

1. Introduction

Magnetoelectric media are those wherein cross effects are observed, i.e. the action of electric fields on the magnetic subsystem of a material and the inverse effect of the magnetic field on the dielectric characteristics or ferroelectric state of the substance. The last case relates to magnetic ferroelectrics or multiferroics [1, 2].

The traditional approach to the study of properties of magnetoelectric substances implies the uniformity of the medium, when the volume of the substance to be investigated represents a single magnetic or ferroelectric domain. This, in turn, implies measurements in sufficiently strong magnetic and electric fields, which polarize the sample to saturation. However, a distinct tendency has recently appeared toward the investigation of materials in a spontaneous state, taking into account the presence of a domain structure in them [3–6], which is connected with the following observations.

• An increasing number of materials synthesized at present falls on thin films, in which, according to the Kittel law, the size of the domains decreases with decreasing thickness of the film. In this case, the volume fraction of the domain walls in the material and their role in the formation of its properties grow noticeably.

• Some magnetoelectric effects can manifest themselves on the scale of separate domains or even domain walls. In this case, the measurement of the integral (averaged over many domains) signal does not give information about these kinds of changes.

• Of special interest are the effects absent in uniform samples, which are connected directly with the domain walls and other inhomogeneities, such as vortices, skyrmions, and Bloch lines.

Thus, the domain walls in ferroelectrics have electrically conducting properties different from the properties of the domains that are separated by these walls. A flurry of interest in this phenomenon arose after the detection of an enhanced conductivity of domain walls in the bismuth ferrite ($BiFeO_3$) multiferroic [7]. (Notice that in ferroelectrics depleted of magnetic ordering the conductivity of the domain walls was theoretically predicted [8] and experimentally discovered [9] considerably earlier.) It is interesting that, even upon displacement of a domain wall, its 'electroconducting image' remains 'imprinted' in the ferroelectric [10], which supposedly is explained by the accumulation of charged defects (oxygen

A P Pyatakov, A S Sergeev, E P Nikolaeva, T B Kosykh, A V Nikolaev
Faculty of Physics, Lomonosov Moscow State University,
Leninskie gory, 119991 Moscow, Russian Federation
E-mail: pyatakov@physics.msu.ru
K A Zvezdin Prokhorov General Physics Institute,
Russian Academy of Sciences,
ul. Vavilova 38, 119991 Moscow, Russian Federation;
Kintech Laboratory Ltd,
3-ya Khoroshevskaya ul. 12, 123298 Moscow, Russian Federation
E-mail: zvezdin@gmail.com
A K Zvezdin Prokhorov General Physics Institute,
Russian Academy of Sciences,
ul. Vavilova 38, 119991 Moscow, Russian Federation,
Lebedev Physical Institute, Russian Academy of Sciences,
Leninskii prosp. 53, 119991 Moscow, Russian Federation

Received 1 July 2015
Uspekhi Fizicheskikh Nauk **185** (10) 1077 – 1088 (2015)
DOI: 10.3367/UFNr.0185.201510k.1077
Translated by S N Gorin; edited by A Radzig

vacancies or dislocations) at the site of the location of domain boundaries.

It should be noted that in some other $R\mathrm{MnO_3}$ perovskites (R is a rare-earth ion) the opposite effect of a decrease in the conductivity in the region of the location of the ferroelectric domain walls can take place (e.g., in yttrium manganite), as can a bi-directional change of conductivity (in holmium manganite), depending on the sign of the related electric charge at the ferroelectric domain wall [5]. The conducting, electrostatic, and hypothetical magnetic properties of the ferroelectric domain walls were considered in special reviews [3, 5].

Considerably less attention is paid to the magnetoelectric properties of magnetic domain walls and other micromagnetic structures, and also to the study of the possibility of controling them with the aid of an electric field. In this case, composite media are considered, as a rule, in which the layer of a usual magnetic material, e.g., permalloy, is deposited onto a piezoelectric substrate. Here, the action of the electric field on the micromagnetic structure is implemented via the mechanical connection between the two layers: strain, which appears as a result of the reverse piezoelectric effect, leads to a reconstruction of the micromagnetic structure caused by magnetostriction phenomena [11–16]. This scheme is promising from a practical viewpoint, since it makes it possible to control the position of magnetic domain walls at room temperatures under the action of small control voltages not exceeding 0.1 V [15].

In single-phase materials, the magnetoelectric properties can also manifest themselves at domain walls, for example, when the magnetic domain walls play simultaneously the role of the boundaries of ferroelectric domains, as occurs in $R\mathrm{FeO_3}$ orthoferrites [17, 18]. Such boundaries are called 'composite' [18], but they should be distinguished from the micromagnetic structures in the composite materials. Unfortunately, this effect appears in orthoferrites only at low temperatures, when the rare-earth magnetic subsystem is ordered. In the recent study [19] covering the multiferroics of another type, CuO and $\mathrm{MnWO_4}$, which are characterized by incommensurate spin structures in the ferroelectric state, the presence of electric polarization at the magnetic domain walls was predicted to exist in the paraelectric phase, but again at low temperatures.

At the same time, there are single-phase materials, e.g., epitaxial films of iron garnets, in which the transformation of the micromagnetic structure induced by an electric field is observed even at room temperature [20–22]. Apart from the practical significance of this high-temperature magnetoelectric (ME) effect, of great fundamental interest is the mechanism of this phenomenon, which to date remains debatable (for greater detail, see Section 3).

When studying the magnetoelectric properties of micromagnetic structures in iron-garnet films, three basic methods of experimental observation can be distinguished; they are given in Fig. 1 in the order of their discovery. Historically, the first was the electromagnetooptical observation technique [26] based on measuring the angle of the Faraday rotation of the plane of polarization of light passed through an iron-garnet film placed between two flat transparent electrodes (Fig. 1a). The application of an AC electric field with a strength of approximately 1 kV cm^{-1} led to a modulation of the angle of rotation of about several seconds or several dozen seconds of arc [23, 24]. Upon focusing the laser beam on the site of the location of the domain wall, the signal caused by the

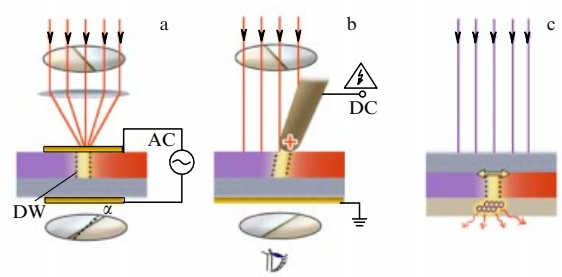

Figure 1. (Color online.) Three methods for observing the magnetoelectric properties in iron-garnet films: (a) electromagnetooptical [23, 24], (b) magnetoelectric probe [20, 21], and (c) spectroscopy of single molecules [25]; α is the angle of the Faraday rotation; AC (DC) stands for the AC (DC) voltage; the red and blue colors designate the magnetic domains with opposite magnetizations. The dotted lines indicate the position of the domain wall (DW). The substrate (gray layer in color version) is at the bottom one in panels 'a' and 'b', and at the top one in panel 'c'.

electromagnetooptical effect grew by more than an order of magnitude in comparison with the same signal from uniformly magnetized domains [24, 27], which indicated the high sensitivity of the domain wall to the action of an electric field.

As the following stage in the study of the ME properties of domain walls was the experiment in which the electric action was localized via the creation of a high-strength field near the pointed tip of an electrode (Fig. 1b). Upon application of a DC voltage to the electrode, an attraction or a repulsion of the wall, depending on the polarity of the applied voltage, was observed [4, 20, 28–33]. In the further development of this procedure, the pointed wire was substituted by a conducting probe of a scanning atomic-force microscope [21, 34], but the resolution upon the application of this method remained restricted by the diffraction limit, since the visualization of the micromagnetic structure was achieved by magnetooptical methods. The problem could be solved via application of the methods of magnetic force microscopy for the visualization of the domain structure, similar to how this is done in experiments on composite structures [11, 12], but this method is not suitable for iron-garnet films because of their small coercive force and the high mobility of the magnetic domain walls: the magnetized needle of the probe entrains the domain wall, making impossible the detection of the electrically induced displacements of the domain wall against this background [21]. Note, however, that a method using combination of electrical action and scanning probe microscopy is successfully employed under the name magnetoelectric force microscopy (MeFM) [35] for the analysis of hard magnetic materials.

Finally, the spectroscopy of single molecules described in the recent article [25] may become the most precise method of measurement of magnetoelectric effects on domain walls. It makes possible studying the distribution of electric fields created by domain walls by measuring the displacement (as a result of the Stark effect) of the frequency of the emission line of the organic dibenzanthanthrene (DBATT) molecule located in a hexadecane layer applied to the surface of an iron-garnet film (Fig. 1c). An AC magnetic field makes the magnetic inhomogeneity move relative to the position of the molecule, leading to the modulation of the frequency of the luminescent emission of the molecule. This method has a sensitivity on the order of 10 V cm^{-1}, and the resolution is determined by the accuracy of the positioning of the

molecular probe relative to the domain wall, i.e., in the limit it can reach an atomic-scale resolution. Note that the method of the single-molecule spectroscopy makes it possible to measure the magnetic-field-induced change in the electric polarization, i.e., the magnetoelectric effect being inverse with respect to that measured by the first two methods.

The above-described methods for investigating the electrostatic properties of domain structures are not only applicable to studying films of iron garnets; they can prove to be also useful in the adjacent fields of the physics of materials, in which the magnetic separation of phases with charge inhomogeneities can occur and stable electrically charged structures of magnetic origin are observed [36] (in the case of opaque materials, the magnetooptical visualization can be implemented using the Kerr effect with light reflection).

The paper outline is as follows. In Section 2, we consider in detail the experimental results of the observation of magnetoelectric effects on micromagnetic structures in epitaxial films of iron garnets obtained with the aid of the second of the methods described above.

In Section 3, theoretical models proposed for describing the phenomenon of electrically induced motion of domain walls are discussed.

In Section 4, results are presented of the numerical simulation of the magnetoelectric properties of micromagnetic objects, which will make it possible to look more broadly at the problem of magnetoelectric phenomena in micromagnetism: not only as the electrically induced motion of domain walls, but also as the electrical control of micromagnetic structures of reduced dimension, such as Bloch lines and Bloch points, as well as skyrmions.

The basic conclusions and an analysis of the prospects for the practical implementation of these effects are given in Section 5.

2. Experimental results

The existence of magnetoelectric properties in micromagnetic structures was first discovered in the form of the displacement of domain walls in films of iron garnets under the action of a static inhomogeneous electric field at the Faculty of Physics of Moscow State University (MSU) in the laboratory guided by A S Logginov [20]. In the subsequent work of this research group, the behavior of a domain wall depending on its shape in samples with different crystallographic orientations of the substrates on which the films were grown was studied [28–30]. Later on, the influence of external magnetic fields on the motion of domain walls caused by an electric field was examined; a change in the direction of the displacement [31], magnitude of the displacement [32], and the velocity of domain wall [33] depending on the strength and direction of the magnetic field was revealed. For the study of the peculiarities in motion of domain walls, a dynamic method was applied, in which the wall is displaced under the action of a pulsed electric field. Furthermore, the specific features of the behavior of domain walls under the action of an electric field created by a stripe-shaped electrode were also studied [37]. The results of the analysis of the properties of domain structures in the electric field of a charged electrode are presented below.

The samples investigated were epitaxial films of iron garnets $(BiLu)_3(FeGa)_5O_{12}$ grown by A M Balbashov in the Moscow Power Engineering Institute by the method of liquid-phase epitaxy on $Gd_3Ga_5O_{12}$ substrates 500 μm thick [38]. The parameters of the samples investigated are given in Table 1 [39].

The general setup of experiments is illustrated in Fig. 2. The electric field was created by applying a constant voltage to a pointed wire of a diamagnetic material. The domain structure was visualized with the aid of the magnetooptical Faraday effect. In the measurements, the position of a domain wall was recorded in the initial state and after the application of an electric voltage to the needle. It was revealed that under the action of the electric field the domain wall was displaced (Fig. 3). After turning off the voltage, the domain wall returned into the initial position. With the change in the polarity of the voltage on the needle, the direction of the displacement became opposite. The direction of the displacement of the domain wall relative to the needle ('attraction' or 'repulsion') was independent of which of the domains the needle was carried from to the wall.

Of special interest is the influence of an electric field on the motion of the stripe domain heads (Fig. 4). In contrast to the boundaries of stripe domains, the heads of stripe domains are in a metastable state, and even upon small changes in the ambient conditions a stripe domain head can become displaced a significant distance. In Ref. [40], we measured

Table 1. Parameters of $(BiLu)_3(FeGa)_5O_{12}$ samples*

No.	Orientation of substrate	h, μm	$4\pi M_s$, G	p, μm	(θ_0, φ_0)	Effect
1	(111)	8.5	63.0	77.0	(0, 0)	Absent
2	(111)	19.0	78.0	39.0	(0, 0)	Absent
3	(110)	4.0	162.0	9.2	(10, −53)	Present
4	(110)	6.0	76.0	14.0	(10, 1.5)	Present
5	(210)	7.4	77.0	44.0	(46, 207)	Present
6	(210)	10.0	62.0	28.0	(46, 189)	Present
7	(210)	10.0	53.5	34.0	(40, 189)	Present
8	(210)	11.0	43.5	36.0	(46, −17)	Present
9	(210)	18.7	62.2	26.0	(50, −203)	Present
10	(111)	10.0	144.0	8.7	(0, 0)	Absent**

* h is the thickness of the film, M_s is the saturation magnetization, p is the period of the domain structure in the undisturbed state, θ_0, φ_0 are the angular coordinates of the magnetization vector in the domains in the coordinate system with the normal to the film as the polar axis and the azimuthal axis along the directions $[\bar{1}10]$ and $[\bar{1}20]$ for the films (110) and (210), respectively.

** Sample No. 10 (of composition $(BiTm)_3(FeGa)_5O_{12}$) was used in the observation of the magnetoelectric (ME) properties of vertical Bloch lines; in the regions of domain walls without vertical Bloch lines, the effect was absent, just as in all samples with the substrate orientation (111) [39].

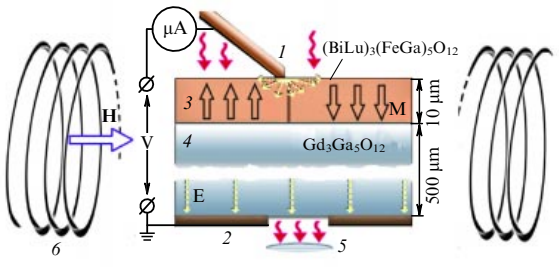

Figure 2. Setup of the experiment: (*1*) electric probe; (*2*) grounded electrode; (*3*) sample; (*4*) substrate; (*5*) optical system of the microscope, and (*6*) magnetizing coils. Wavy arrows mark laser radiation [28].

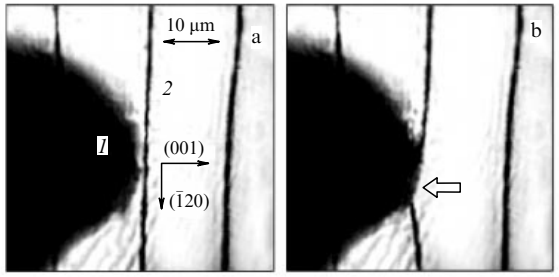

Figure 3. Magnetooptical image of the film in a transmitted light: (a) (*1*) pointed wire made of a diamagnetic metal (in this case, of copper); (*2*) image of the domain wall; (b) the displacement of the domain wall under the effect of a potential that is positive relative to the substrate applied to the needle [20].

the dependence of the displacement of a domain head on the voltage at the needle. It was shown that in the range of voltages up to 1 kV the displacement of the domain wall grows almost linearly, and with a further increase in the voltage, the growth of its displacement is saturated. It can be assumed that this is connected with a rapid decrease in the strength of the electric field upon moving away from the probe and with a notable increase in the magnetostatic energy because of the strain of the domain.

In order to investigate the electrically induced motion of domain heads, the method of high-speed photography was utilized [28]. A specific feature of the method was that voltage was applied to the needle in the form of a square pulse with a duration of 300 ns and with a pulse-rise time of 20 ns, and an instantaneous photograph of the domain structure was obtained using illumination with a 10-ns laser pulse. By

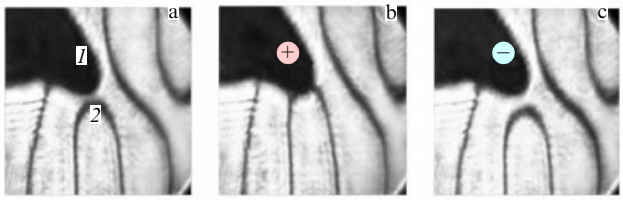

Figure 4. Magnetooptical observation of the action of an electric field on the heads of magnetic domains (sample No. 8 in Table 1): diffuse dark lines are the images of domain walls; (a) (*1*) image of the electrode (probe); (*2*) head of a magnetic domain; (b) attraction of the head to the needle at a potential that is positive relative to the substrate; (c) repulsion of the head from the needle at a negative potential [30].

changing the time of the delay between the pulse of the electric voltage and the laser pulse, it was possible to observe the sequential phases of the motion of the domain wall. This dynamic method made it possible to measure the velocity of motion of the domain heads and its dependence on the electric field (Fig. 5).

The effect of the displacement of the domain walls was most pronounced in films grown on substrates with a crystallographic orientation (210); noticeable, but smaller displacements were observed in the (110) samples. In the (111) films, no displacements of domain walls under the action of an electric field were revealed.

It should be noted that the domain structure in the films of iron garnets grown on substrates with crystallographic orientation (111) investigated in Refs [20, 28] was of a labyrinth type; the magnetization in the domains was directed perpendicularly to the film. The domain structure in the samples with the substrate crystallographic orientations (110) and (210) transformed into a stripe structure as a result of the location of the easy axis in the plane of the film (orthorhombic anisotropy). Because of the combined action of cubic, orthorhombic, and uniaxial anisotropies, the direction of the magnetization in the domains of the (110) and (210) samples was not perpendicular to the film and was assigned by the angles in the spherical coordinate system, θ_0 and φ_0; θ_0 is the polar angle counted from the normal to the film, and φ_0 is the azimuthal angle measured from the direction $[\bar{1}10]$ for (110) films, and from the direction $[\bar{1}20]$ for (210) films (Fig. 6a).

In the (210) and (110) samples, an in-plane magnetic field changes the stripe domain structure. The domains with one direction of magnetization become wider than those with the opposite direction; the domain structure becomes distorted, or, at a sufficiently large value of the in-plane field, the iron-garnet film is transformed into a single-domain state. The in-plane DC magnetic field also affects the magnetoelectric properties of the domain walls, leading to giant (on the order of the domain width) electrically induced displacements of the domain walls [31 – 33]. This is most clearly noticeable in cases where the field is perpendicular to the plane of the domain wall.

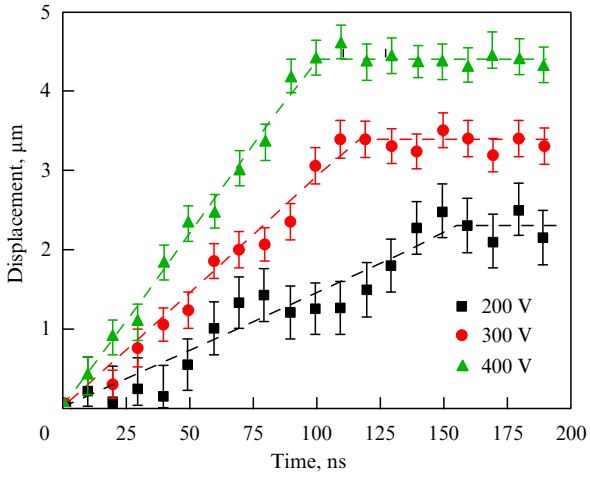

Figure 5. Time dependence of the displacement of a domain head at different values of the potential at the electrode (sample No. 6, see Table 1) [28].

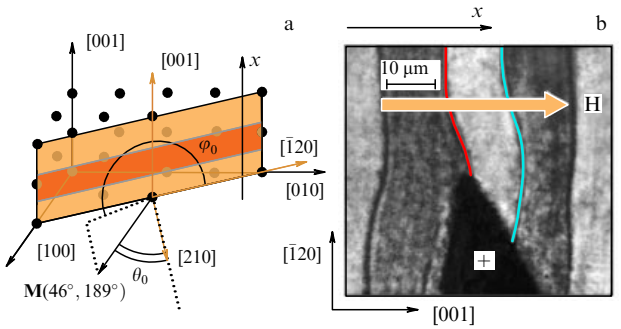

Figure 6. (Color online). (a) Direction of the magnetization vector in the domains of the (210) sample in sample No. 6 (see Table 1); (b) displacement of a domain wall in the (210) sample [32].

The magnetooptical image given in Fig. 6b demonstrates the displacement of the domain wall under the action of a positively charged electrode in the presence of a magnetic field. In the equilibrium state, the domain walls lie along the direction [$\bar{1}$20]. In the absence of a magnetic field, the direction of the displacement of the domain wall is determined only by the sign of the voltage applied to the needle.

An external magnetic field applied in the plane of the film perpendicular to the domain wall substantially changes the character of the observed effect. In particular, the displacement of the domain walls grows at a sufficiently large strength of the magnetic field, and its direction relative to the needle begins alternating from wall to wall.

The dependence of the displacement of the domain wall on the magnetic field with a DC voltage at the needle was measured for two adjacent domain walls in the sample with a crystallographic orientation (210) (walls 1 and 2 in Fig. 7). The positive value of the displacement corresponds to the attraction of the wall to the needle, and the negative value to the repulsion of the wall from the needle. The positive and negative values of the magnetic field correspond to the field direction along the x-axis and in the opposite direction, respectively. In the absence of a magnetic field, the displacement of both walls is positive; the displacement of the domain wall monotonically increases or decreases in proportion to a change in the magnetic field strength in either side. For each domain wall, there is a critical value H_c of the magnetic field at which the wall does not react to the electric field (in Fig. 7, $|H_c| = 25 \pm 5$ Oe).

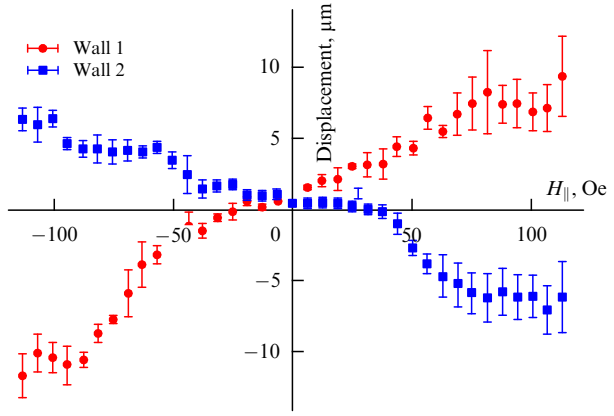

Figure 7. Displacement of the domain wall for sample No. 7 (see Table 1) from the equilibrium position under the action of an electric field depending on the value of the external magnetic field applied in the film plane. Voltage at the needle is 1500 V. The two branches correspond to two adjacent domain walls [32].

To increase the electrically induced displacement of the domain head, a magnetic field was applied along the stripe domain and perpendicularly to the wall of the head [i.e., along the [$\bar{1}$20]-axis in the sample with the crystallographic orientation (210)]. Figure 8 plots the dependence of the displacement of the domain head under the action of an electric field on the strength of the in-plane magnetic field [40]. The data are presented for two types of domain heads, similar to how this was done for the two types of domain walls in paper [28]. From a comparison of the graphs given in Figs 7 and 8, it can be seen that the direction of the motion of the domain head caused by the electric field can change depending on the value and direction of the field in the film plane (just as in the case of the straight segments of the domain walls). The values of the critical switching fields for the heads are approximately three times higher than for the straight segments of the wall. Furthermore, the change in the direction of the motion of the domain head is not accompanied by a further growth of the absolute value of the displacement (see the region of negative displacements in Fig. 8).

The magnetoelectric effect appears under the action of an electric field not only on the domain walls but also on the micromagnetic structures in the domain walls themselves — vertical Bloch lines (VBLs). A visualization of the regions of domain walls with VBLs was carried out using the dark-field method [41] (observation method in which only the light scattered from inhomogeneities falls into the microscope objective) in the iron-garnet film $(BiTm)_3(FeGa)_5O_{12}$ with a crystallographic orientation (111) [39] (sample No. 10 in Table 1). A VBL is identified as the region of a domain wall with a changed contrast (lighter or darker regions). Under the action of the electric field from the charged needle, the VBLs are displaced along the domain wall. No systematic dependence of the direction and magnitude of the VBL displacement on the polarity and value of the electric voltage was observed, which is probably connected with the (unestablished) internal structure of the Bloch lines.

Besides the study of the action of a point electrode on the micromagnetic structure, the study of the influence of the electric field caused by the electrodes of other geometries, in particular, of the 'charged line' type, is also of interest. In

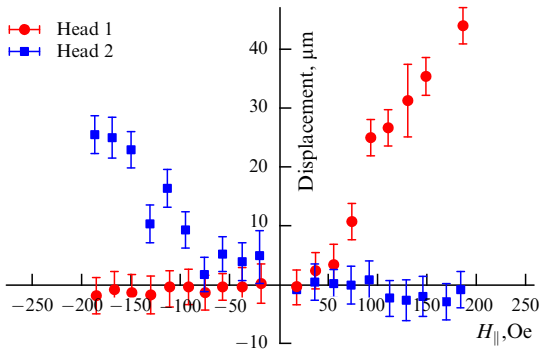

Figure 8. Displacement of a domain head under the action of an electric field depending on the magnetic field strength in the plane of sample No. 5. Voltage at the needle $U = 1$kV [40].

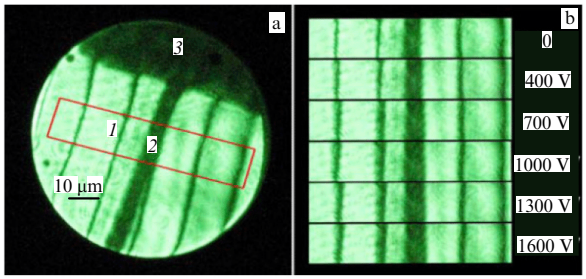

Figure 9. Magnetooptical images of a domain structure in an iron-garnet film subjected to the action of an electric field: (a) (*1*) domain wall; (*2*) stripe electrode; (*3*) contact area, and (b) magnetooptical images of the region outlined by a rectangle in (a) at different values of the voltage at the electrode. Sample No. 9 (see Table) [37].

paper [37], the results of experiments performed on an iron-garnet film with a system of strip palladium electrodes applied by the photolithographic method onto its surface are described. A high voltage was applied between the electrode and the substrate; observations of the micromagnetic structure of the sample were performed by the magnetooptical method in the transmitted light (Fig. 9a).

When the strip electrode was parallel to the domain walls, a broadening of the images of the domain walls was observed, which monotonically increased threefold with an increase in the voltage from 0 to 1600 V (Fig. 9b). This change in the visible width of the domain wall can be interpreted as being due to the tilting of the plane of the domain wall by an angle of $\approx 10^\circ$. In this case, the domain walls (except for the wall that is nearest to the electrode) are barely displaced toward the electrode, in contrast to the case of a point probe; this is, apparently, explained by the tendency of the domains to retain their sizes unaltered.

3. Theoretical interpretation of the results

3.1 Possible mechanisms of the domain wall displacement effect

The observed features of the displacement of domain walls under the action of an electric field make it possible to assert that this effect is of magnetoelectric origin. Phenomena of other nature can be excluded on the basis of symmetry considerations [20]: the magnetostriction caused by the pressure of the electrode on the film would not depend on the polarity of the voltage, and the magnetic fields created by electric currents would attract or repulse the wall depending on which of the domains the needle is located above, thus contradicting the results of the experiments.

At present, two mechanisms of a magnetoelectric nature have been suggested to explain the observed phenomenon: inhomogeneous magnetoelectric interaction [20], and a variation of the magnetic anisotropy constants under the action of an inhomogeneous electric field [42]. These mechanisms correspond to different 'inhomogeneities': in the first case, we are dealing with an inhomogeneous distribution of the magnetization vector inside the domain wall, and in the second case we have an inhomogeneity of the electric field created by a needle-shaped electrode. Let us examine these effects in more detail.

The necessary condition for the emergence of electric polarization is the central symmetry breaking. If the center of inversion is absent from the symmetry group of the crystal lattice, the crystal can possess spontaneous polarization, i.e., ferroelectric properties. However, the breaking of the central symmetry can be realized in any magnetic crystal, merely due to the formation of a micromagnetic structure. Thus, if a micromagnetic structure breaks the central symmetry in a certain region of the crystal, then in this region an associated electric polarization can arise. This is the heart of the idea of an inhomogeneous magnetoelectric interaction [1, 43, 44] (which is also called the flexomagnetoelectric effect, in view of the similarity with the flexoelectric effect in dielectrics and liquid crystals [22, 39]).

The symmetry of the micromagnetic structure of a domain wall is determined by the geometry of the distribution of the magnetization vector. There are two basic types of domain walls: a Bloch wall, in which the rotation of the vector of magnetization occurs in the plane of the domain wall, and a Néel wall, in which the rotation occurs in the perpendicular plane. A Bloch type domain wall cannot possess electric polarization, since its 'screw' geometry is centrally symmetric. On the contrary, a 'fan-shaped' Néel wall can possess electric polarization [43, 45] and, therefore, can be displaced under the action of an inhomogeneous electric field [46, 47].

The second mechanism involves the electric field deforming the crystalline cell: it displaces the ions and the clouds of the electron density, which results in changes in the magnetic anisotropy constants [21]. If the electric field possesses a strong spatial inhomogeneity, a change in the anisotropy constants will also be inhomogeneous. This will lead to the appearance of a force which acts on any micromagnetic object.

Also connected with this phenomenon is a linear magnetoelectric effect in the films of iron–yttrium garnet in a uniform electric field [24, 27]. The object of direct measurements here is the change in the angle of the Faraday rotation under the action of an electric field (Fig. 1a). In the presence of a magnetic field, which tilts the vector of magnetization in the domains, a change in the anisotropy constants must lead to displacements of the walls even in a uniform electric field. According to paper [27], the displacement of a domain wall at the strengths of the electric and magnetic fields $E = 10^7$ V m^{-1} and $H = 300$ Oe can be estimated to be equal to 0.01 μm. The relative change in the anisotropy constants under the action of the electric field $E = 1.2 \times 10^6$ V m^{-1} is 4×10^{-5} [23].

In Sections 3.2 and 3.3, it will be shown that both these mechanisms provide a qualitative explanation of the behavior of the domain walls under the action of an electric field in the presence of a magnetic field in the plane of the film.

3.2 Inhomogeneous magnetoelectric interaction

The distribution of the electric polarization **P**, which appears in the region of a nonuniform distribution of the magnetization vector **M** as a result of the inhomogeneous magnetoelectric effect, is described by the following equation [45, 48]

$$\mathbf{P} = \gamma\chi_e\left[(\mathbf{M}\nabla)\,\mathbf{M} - \mathbf{M}(\nabla\mathbf{M})\right], \qquad (1)$$

where γ is the magnetoelectric interaction coefficient, and χ_e is the dielectric susceptibility. The force that the electric field exerts on the domain wall is determined by the surface bound electric charge. The linear density of the bound charge along the wall is defined as $q = \int P_z\,\mathrm{d}x$, where the x-axis is directed perpendicularly to the domain wall. This integral has a simple geometric interpretation. Let us go

from the integral to a discrete sum over the neighboring magnetization vectors:

$$\int P_z \, \mathrm{d}x \sim \int \left(M_x \frac{\partial M_z}{\partial x} - M_z \frac{\partial M_x}{\partial x} \right) \mathrm{d}x = \int \left[\frac{\partial \mathbf{M}}{\partial x} \times \mathbf{M} \right]_y \mathrm{d}x = \sum_i \left[\frac{(\mathbf{M}_{i+1} - \mathbf{M}_i)}{\Delta x_i} \times \mathbf{M}_i \right]_y \Delta x_i = \sum_i \left[\mathbf{M}_{i+1} \times \mathbf{M}_i \right]_y . \quad (2)$$

The sum obtained is equal to $2S$, where S is the area swept by the magnetization vector $\mathbf{M}(x)$ in the xz plane in the motion along the x-axis inside the domain wall. The sign of an element of the area for each segment of the trajectory is determined by the direction of going around the origin in this region.

It should be noted that the samples in which a displacement of domain walls is observed possess a 'low-symmetry' crystallographic orientation (210) and (110); therefore, the easy axis in them does not coincide with the normal to the film surface. These samples are also characterized by a complex magnetic anisotropy: apart from the cubic anisotropy, it includes growth-induced and orthorhombic anisotropies [49]. Therefore, the domain walls in these samples possess a complex micromagnetic structure and belong to neither the Bloch nor Néel types. Furthermore, the anisotropy energy substantially exceeds the energy of the demagnetizing fields, which makes it possible to ignore the action of these fields and take advantage of the one-dimensional model of the domain wall.

The trajectories described by the endpoint of the magnetization vector in two adjacent domain walls are shown in Fig. 10a. The black and white circles mark the positions of the magnetization vector in the domains. We assume that the domain walls have identical chirality, which corresponds to the identical direction of the trajectory detour around the origin. Then, at $H = 0$, all the walls possess surface bound electric charges of the same sign.

An in-plane magnetic field will lead to the tilting of the magnetization vector in the domains and to the distortion of the micromagnetic structure of the domain wall. In a sufficiently strong field, the charges of both the walls grow in absolute value, and the charge of one of them changes sign (Fig. 10c). Since the area swept by the magnetization vector changes continuously with a variation of the trajectory, at a certain value of the magnetic field the surface bound charge of one of the walls will become zero (Fig. 10b). If the magnetic field is directed in the opposite direction, the domain walls will 'change their roles', in agreement with experimental data.

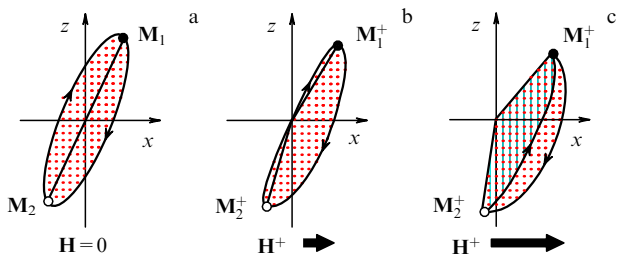

Figure 10. Calculation of the linear density of the electric charge of a domain wall. The arrows show the trajectories of the ends of the magnetization vector in two adjacent domain walls. The black and white circles mark the directions of the magnetization vector in the domains. The different types of hatching correspond to surface electric charges of different signs. The z-axis is directed along the normal to the film, and the x-axis from one domain to another.

Thus, within the framework of the hypothesis of inhomogeneous magnetoelectric interaction, the observed features of the motion of domain walls can be explained on the basis of the following assumptions:

(1) the domain walls are neither Bloch nor Néel types and are characterized by nonzero areas swept by the trajectory of the magnetization vector in the xz plane;

(2) all domain walls originally possess identical chiralities.

As has already been noted, assumption (1) with a great probability corresponds to reality. Assumption (2) can be substantiated by the disturbance of the central symmetry in the process of crystal growth and by the appearance of a uniform spontaneous polarization, which determines the chiralities of the domain walls. Indeed, domain walls of different chiralities are degenerate in terms of the magnetic energy, and even small disturbance can be sufficient for one of the chiralities to become preferable. However, at present there are no experimental data that could confirm the emergence of such a polarization in the samples.

3.3 Variation of anisotropy constants

The contribution to the free-energy density, which corresponds to a change in the anisotropy constants under the action of an inhomogeneous electric field, takes the form [21]

$$w = f_{ijkl} M_i M_j \frac{\partial E_k}{\partial x_l} , \quad (3)$$

where the tensor f_{ijkl} together with the derivative of the strength of the electric field assign a spatially nonuniform distribution of anisotropy constants (Einstein's summation rule is assumed). The force acting on the domain wall is determined by the change in the energy of the system upon the displacement of the wall from its current position.

Since the anisotropy energy is quadratic in the components of the magnetization vector, domain walls of different chiralities possess micromagnetic structures that are identical to within the replacement $\mathbf{M}(x) \to -\mathbf{M}(x)$ (within the framework of the one-dimensional model, with no demagnetizing fields). Consequently, contribution (3) is also independent of the chirality of the wall. The behavior of the wall under the action of an electric field, i.e., attraction or repulsion, will be determined exclusively by the sign of the components of the tensor f_{ijkl} and by the sign of the electric potential applied to the needle. We designate the appropriate contribution to the force that acts on the wall as F_1.

Since the derivatives of the magnetization vector do not enter into expression (3), the magnetoelectric properties of the domain wall within the framework of this mechanism are no longer characterized by a universal dependence on the type of micromagnetic structure. A change in contribution (3) upon a distortion of the distribution of the magnetization vector under the action of a magnetic field will be determined by the relationship between the components of the tensor f_{ijkl}. Nevertheless, some universal factor can be distinguished which will make it possible to reproduce the characteristic properties of the behavior of domain walls in a magnetic field — tilting of the magnetization vector in the domains.

The magnetic field leads to a deflection of the magnetization vector in domains from the easy-axis direction; therefore,

the domains cease being equivalent from the viewpoint of expression (3). This nonequivalence indicates the appearance of a contribution to the force that acts on the domain wall. The value of this contribution (which is connected with the change in the volume of the domains) is directly connected with the strength of the magnetic field, and the sign alternates from wall to wall. Consequently, the addition of this contribution to the force F_1, which acts on all the walls equally, will lead to an increase in the displacement of some walls and to a decrease in the displacement of others up to the zero value with the subsequent passage into the negative region.

In summary, this mechanism also makes it possible to explain the observed displacement of domain walls, and it is impossible to distinguish its manifestations from those of the inhomogeneous magnetoelectric effect on the basis of only experimental data given in Section 2 (as to new experimental facts in support of the theory of the magnetoelectric effect, see Section 5).

4. Low-dimensional micromagnetic structures

4.1 Bloch lines and Bloch points

The domain walls in the films of iron garnets with orientation (111) can possess a rich internal structure [50–53]. If a Bloch type wall contains regions with different chiralities, these regions will be separated by a linear topological defect — a Bloch line (the existence of such an object was recently predicted in ferroelectric domain walls as well [54]). Under the action of demagnetizing fields, the direction of the magnetization vector in different parts of the Bloch line can become different. In this case, these parts will be separated by the so-called Bloch point — by a point defect, which is a discrete analog of a magnetic monopole. If the mechanism that causes the displacement of domain walls is based on an inhomogeneous magnetoelectric interaction, it is natural to assume the presence of magnetoelectric properties in vertical Bloch lines and Bloch points.

A vertical Bloch line represents a Néel type segment in a Bloch domain wall; therefore, it can possess electric polarization. The results of calculations according to formula (1) show that the integral magnitude of the electric charge of a Bloch line on one of the surfaces of a film is $Q = \gamma\chi_e M_s^2 \pi^2 \Lambda$, where Λ is the parameter of the Bloch line width. Substituting into this formula the values of parameters typical of iron garnets yields $Q \approx 4e$, where e is the electron charge.

Figure 11 demonstrates a hypothetical scenario of the switching of the electric dipole of the surface charges in a Bloch line via the introduction and propagation of a Bloch point that possesses a charge equal to $2Q$.

Notice that at present the structure and dynamics of the Bloch point are attracting the attention of many researchers. A specific feature of this object is the singular nature of the distribution of the magnetization vector, which leads, in particular, to the appearance of a force of friction upon motion through the crystal lattice [56], and requires a special approach for a correct numerical simulation [57].

4.2 Skyrmions

The most compact micromagnetic objects with a smooth distribution of the magnetization vector are skyrmions, i.e., magnetic solitons possessing a cylindrical symmetry [58–60]. Skyrmions, just like domain walls, are topologically stable solitons. Similarly to how the structure of domain walls is determined by the local competition between the energy of the exchange interaction and the anisotropy energy, the stability of skyrmions is determined by the competition between the exchange interaction and Dzyaloshinskii–Moriya interaction [61]. This is a key difference between skyrmions and other cylindrically symmetrical structures (vortices and cylindrical magnetic bubbles), whose stability is ensured by 'long-range' dipole–dipole interaction.

The hexagonal lattice of skyrmions was experimentally revealed in helimagnetic MnSi [62], whose crystal structure is characterized by a certain chirality. The role of the chirality of the lattice is clearly reflected in the image of the interface between two grains of a polycrystalline sample of FeGe [63] obtained with the aid of Lorentz electron microscopy (schematically shown in Fig. 12c). The inversion of the brightness indicates the change in the chirality of the skyrmions, which is determined by the sign of the Dzyaloshinskii–Moriya interaction differing in adjacent grains. The skyrmions in these crystals possess a 'Bloch' structure, i.e., the radial component of the magnetization vector is equal in them to zero (Fig. 12a).

Skyrmions are considered promising objects for use in magnetic memory devices [64]. Partly, this is due to the presence of uncommon transport properties in skyrmions.

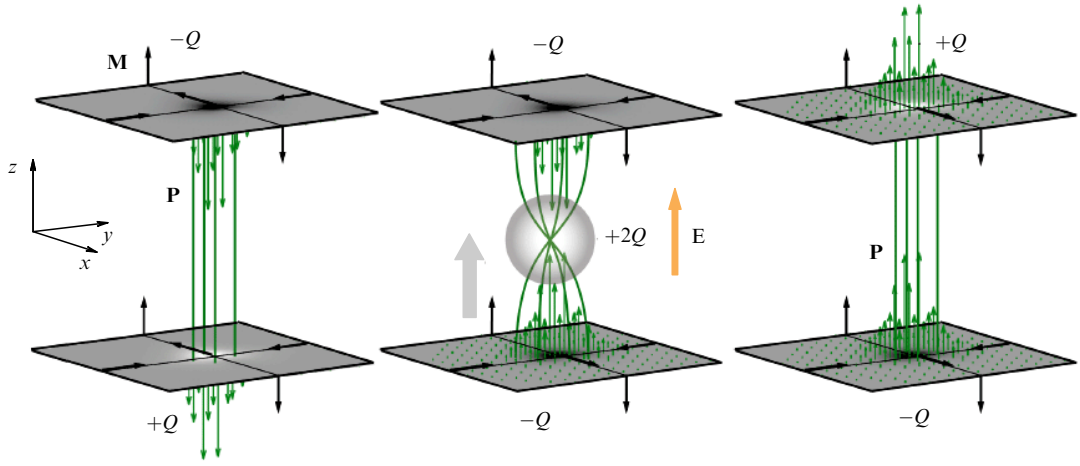

Figure 11. Possible scenario of the switching of the electric polarization of a vertical Bloch line under the action of an electric field by means of the motion of a Bloch point. The x-axis is directed from one domain toward another, and the yz plane coincides with the plane of the domain wall [55].

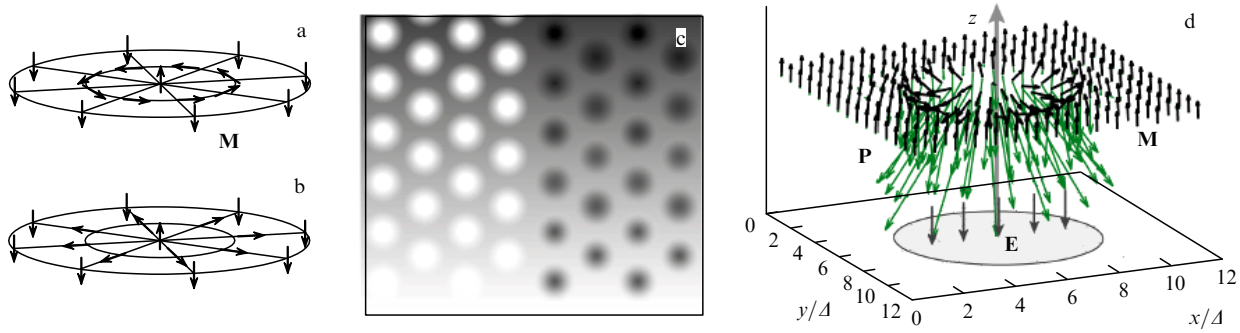

Figure 12. (Color online.) (a) Skyrmion with a Bloch structure; (b) skyrmion with a Néel structure, (c) skyrmion lattice in a polycrystalline sample of FeGe, and (d) skyrmion stabilized by an electric field in a crystal with inhomogeneous magnetoelectric interaction. $E \approx 10^6$ V cm^{-1} is the electric field strength; **P** is the magnetically induced polarization, and $\Delta = \sqrt{A/K}$ is the parameter of the domain wall width. Black arrows mark the distribution of the magnetization in the skyrmion, and green arrows specify the corresponding distribution of the electric polarization [6].

In view of the topologically nontrivial distribution of the magnetization vector, an electron that moves through a skyrmion acquires a Berry phase and experiences the action of effective electric and magnetic fields [65]. This results in a decrease in the strength of the spin-polarized current necessary for moving skyrmions in an MnSi sample by five–six orders of magnitude in comparison with the similar value for domain walls [66].

The control of micromagnetic objects with the aid of an electric current is not optimum from the viewpoint of Joule losses. Therefore, it is of interest to provide the movement of skyrmions by applying an electric field. The first magnetoelectric material in which skyrmions were revealed was Cu_2OSeO_3 [67]. The microscopic mechanism, which couples the polarization and magnetization in this crystal, was called d–p hybridization [68, 69]. However, Cu_2OSeO_3 is not a multiferroic in the strict sense of this word, since it does not possess a ferroelectric order [70]. The polarization in it appears under the action of a magnetic field, which makes it possible to speak of a magnetoelectric effect; however, the spontaneous polarization that can be switched by an electric field was not revealed in it.

Data has recently appeared on the existence of skyrmions in a crystal whose lattice is characterized by a polar symmetry; it is precisely such a crystal that was considered in the first theoretical work devoted to magnetic skyrmions [58, 59]. The skyrmions in the magnetic GaV_4S_8 semiconductor, which is characterized by a rhombohedral symmetry, are 'Néel' type structures, i.e., the magnetization vector 'unfolds' in them in the plane that contains the radial direction (Fig. 12b) [71]. In contrast to helimagnets, in which the plane of the lattice of skyrmions is perpendicular to the external magnetic field, in GaV_4S_8 this plane is perpendicular to the anisotropy axis.

Furthermore, the GaV_4S_8 crystal is a multiferroic, which follows from a change in the electric polarization that accompanies magnetic phase transitions, including the formation of a skyrmion lattice [72]. The microscopic mechanism, which ensures magnetoelectric interaction, appears to be of an exchange-striction type. Although the described effects have thus far been observed only at low temperatures ($T < 13$ K), these investigations are an important stage in the search for the possibility of electric control of magnetic skyrmions. The following stage can become electric field-induced nucleation and subsequent stabilization of the Néel skyrmion in a crystal with an inhomogeneous magnetoelectric interaction (Fig. 12d) [6].

4.3 Magnetic vortices

In structured materials, where the magnetic phase forms so-called nanodots, i.e., disk-shaped regions of a nanometer size, the micromagnetic configuration with the smallest energy is a magnetic vortex, in which the magnetization everywhere, except the central region, lies in the plane of a magnetic nanoparticle. The central region is called the core of the vortex.

The magnetic vortex, being a magnetic inhomogeneity with nonzero spatial derivatives entering into the expression for the magnetoelectric polarization (1), can also experience the action of an electric field. As was predicted by Meshkov et al. [73], an electric field is capable of stabilizing a vortex distribution of the magnetization even if the initial distribution corresponded to a uniformly magnetized particle (Fig. 13). In numerical simulation, the particle size was assumed to be equal to 100 nm (on the order of the exchange length for a medium with the magnetization equal to several dozen gausses and with the order–disorder transition temperature of approximately 500 K) in order that the spontaneous state of the particle would correspond to the uniformly magnetized state. The control electric field in the model was created by a 5-nm wire passing through the center of the particle perpendicular to its plane (see Fig. 13).

The corresponding calculations were carried out with the aid of a SpinPM program package for micromagnetic simulation [74], which was modified by taking into account the contribution to the effective magnetic field introduced by

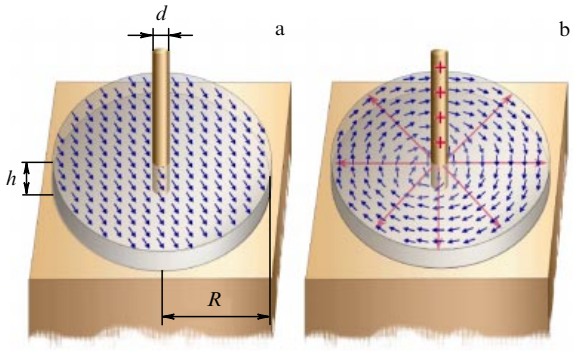

Figure 13. Simulation of the electrically induced nucleation of a vortex at a nanopoint: $d = 5$ nm, $R = 120$ nm, and $h = 10$ nm: (a) uniformly magnetized state, and (b) vortex structure [73].

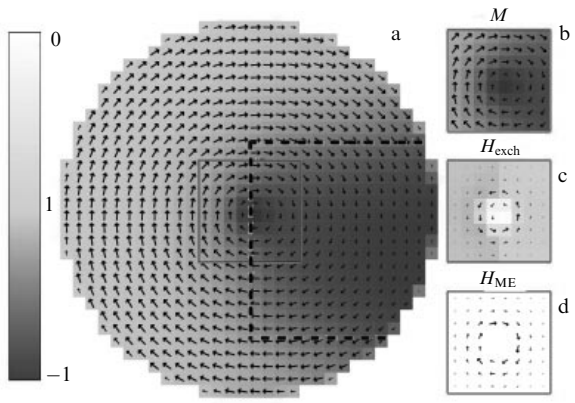

Figure 14. (Color online.) (a) Distribution of magnetization in a nanopoint; the region outlined by the dashed line is a zone with an easy-axis anisotropy (defect); (b–d) distributions of (b) magnetization M, (c) effective exchange field H_{exch}, and (d) effective magnetoelectric field H_{ME} in the region of the vortex core; the x and y components are indicated by arrows, and the z component is shown by color [73].

the inhomogeneous magnetoelectric interaction:

$$H_i^{ME} = \gamma\chi_e \left[2(E_i\nabla_j M_j - E_j\nabla_i M_j) - M_j(\nabla_i E_j - \nabla_j E_i)\right]. \quad (4)$$

The distribution of the effective magnetoelectric field H_{ME} corresponding to a vortex state is presented in Fig. 14d. The effective magnetoelectric field H_{ME} stabilizes the vortex state, while the effective field of the exchange interaction H_{exch} (Fig. 14c) attempts to untwist the vortex. Since in the ideal particle with a uniformly magnetized state the effective field (4) is identically equal to zero, to nucleate a vortex we used an artificial defect created by means of a local change in the anisotropy constant from the easy-plane to easy-axis type (see Fig. 14).

The calculated values of the control voltages, which switched the particle from the vortex state to the uniform state and back, were about 100 V; however, by selecting the size of the particle or of the amount of the spontaneous magnetization via the balance between the magnetostatic dipole–dipole and exchange interactions, it was possible to attain the appearance of metastable states at the strength of the electric field close to zero (for particles of the given sizes, the magnetization in this case must be equal to 150 G [73]).

5. Conclusions

The magnetoelectric effect on the domain walls in films of iron garnets is the prototypical example of the manifestation of appropriate effects in the micromagnetic structures of single-phase materials. This effect is observed at room temperatures and atmospheric pressures, which can be of practical interest for applications in spin electronics, magnonics, and magnetoplasmonics. At present, in these branches of technology, methods based either on the generation of magnetic fields with the aid of inductive elements or on the effect of the transfer of a spin torque during the flow of a spin-polarized current through a magnetic medium are used to control the magnetic state of elements [75]. Both methods imply extremely high densities of current flowing through a nanoelement ($10^6 - 10^7$ A cm^{-2}). At the same time, the potential of magnetoelectric control makes it possible to realize the electrostatic principle of action, similar to that utilized in field-effect transistors. This will make it possible to radically reduce the electric current density and to substantially decrease the energy consumption [76]. The latter depends on the magnitudes of the control voltages, which so far remain too great for electronic applications (in the experiments described in Section 2, the displacements of domain walls noticeable in an optical microscope were achieved at voltages applied to the point electrode that reached several hundred volts).

A substantial decrease in the control voltages and in the energy of switching the magnetic state can be reached via a miniaturization of the electrode, since in this case the field strength increases significantly. A considerable strengthening of the effect of the magnetoelectric action (by an order of magnitude or more; see Figs 7, 8) can be reached by the application of additional magnetic fields created with the use of permanent magnets, which do not consume energy. The selection of the 'operating point', at which the basic micromagnetic forces, i.e., the exchange interaction trying to convert the system into a uniform magnetized state, and the magnetostatic dipole–dipole interaction generating magnetic inhomogeneities, balance each other also allows triggering the first-order phase transition from the uniform state into the inhomogeneous state and back by utilizing the small action of an external electric field [73].

The mechanism of the action of the magnetoelectric effect at the domain walls in iron-garnet films remains a debated issue. Both hypotheses considered in Section 3, i.e., the electric polarization induced by magnetic inhomogeneities (inhomogeneous magnetoelectric interaction) [4, 43, 77] and the local variation of the magnetic anisotropy induced by an inhomogeneous electric field at the site of location of the needle [21, 42], make it possible to explain the basic features of the effects described in Section 2. At the same time, detection (by the single-molecule spectroscopy method) of the electric field connected with magnetic inhomogeneities in the films of iron garnets [25] counts in favor of the first mechanism. A decisive experiment which could distinguish one mechanism from another could be the direct observation of the direction of the magnetization rotation in the domain wall and its relation to the effect of the electrically induced displacement of the walls. Unfortunately, the conduction of such experiments presents great difficulties because of the negligibly small volume occupied in the sample by domain walls (the thickness of a domain wall is on the order of 100 nm at the domain width of 10 μm), which does not make it possible to use the traditional methods of polarized neutron scattering.

The mechanism of inhomogeneous magnetoelectric interaction can also produce some other effects that were theoretically predicted, but still have not been confirmed experimentally:

- the transformation (under the action of an electric field) of the micromagnetic structure of a domain wall from a Bloch wall type to a Néel wall type [78], which must manifest itself in the dynamics of domain walls under the action of a magnetic field in the form of a delay of the onset of the Walker breakdown and of a notable increase in the velocity of motion of the domain wall [79–81];
- the influence of an electric field on the mobility of Bloch lines [82] and on the dynamics and structure of Bloch lines within the domain walls of antiferromagnets [83]. It can be supposed that the most clearly pronounced effect of an electric field would be manifested during its influence on clusters of Bloch lines, in which the total angle of the

magnetization rotation is $N\pi$, where N is the number of lines in the cluster. Such clusters are formed during the motion of a domain wall [51, 53];

• the switching of the direction of the magnetization rotation in the domain wall under the action of an electric field [37, 78];

• the pinning of magnetic domain walls at the ferroelectric domain walls in multiferroics [84, 85] and the presence of a micromagnetic structure in the ferroelectric domain walls in multiferroics [86];

• the nucleation of a magnetic inhomogeneity (including a domain wall [46]) under the action of an electric field. Under the conditions of experiments described in Section 2, the required electric fields are sufficiently large (by an order of magnitude higher than those usually employed in experiments), but they can be substantially lowered when working in the region near the spin-reorientation phase transitions [52];

• the switching of the state of a magnetic nanoparticle from a vortex state to a uniform state (see Section 4.3) and to an antivortex [4, 87] state;

• the stabilization of a single skyrmion in an electric field and electric action on the Bloch point (see Section 4.1).

As we see, the list of problems is rather long, and they can compose a program for further studies in the field of micromagnetism in the near future.

Acknowledgments

This work has been partially supported by the Russian Foundation for Basic Research (project Nos 13-02-02443 ofi_m2, and 14-29-08216 ofi_m), and by the Ministry of Education and Science of the Russian Federation (project REMEFI57614X0023). A P P, K A Z, and A K Z are also thankful for the support from the joint Russian–Turkish program with assistance of the Russian Foundation for Basic Research (No. 14-02-91374 ST_a) and TUBITAK (No. 213M524).

References

1. Smolenskii G A, Chupis I E *Sov. Phys. Usp.* **25** 475 (1982); *Usp. Fiz. Nauk* **137** 415 (1982)
2. Pyatakov A P, Zvezdin A K *Phys. Usp.* **55** 557 (2012); *Usp. Fiz. Nauk* **182** 593 (2012)
3. Catalan G et al. *Rev. Mod. Phys.* **84** 119 (2012)
4. Pyatakov A P, Meshkov G A, Zvezdin A K *J. Magn. Magn. Mater.* **324** 3551 (2012)
5. Matzen S, Fusil S *Comptes Rendus Phys.* **16** 227 (2015)
6. Pyatakov A P et al. *J. Magn. Magn. Mater.* **383** 255 (2015)
7. Seidel J et al. *Nature Mater.* **8** 229 (2009)
8. Vul B M, Guro G M, Ivanchik I I *Ferroelectrics* **6** 29 (1973)
9. Grekov A A, Adonin A A, Protsenko N P *Ferroelectrics* **13** 483 (1976)
10. Stolichnov I et al. *Appl. Phys. Lett.* **104** 132902 (2014)
11. Chung T-K, Carman G P, Mohanchandra K P *Appl. Phys. Lett.* **92** 112509 (2008)
12. Chung T-K, Keller S, Carman G P *Appl. Phys. Lett.* **94** 132501 (2009)
13. Brintlinger T et al. *Nano Lett.* **10** 1219 (2010)
14. Lei N et al. *Nature Commun.* **4** 1378 (2013)
15. Chen H T, Soh A K *Mater. Res. Bull.* **59** 42 (2014)
16. Petrov V M, Srinivasan G *Phys. Rev. B* **90** 144411 (2014)
17. Zvezdin A K, Mukhin A A *JETP Lett.* **88** 505 (2008); *Pis'ma Zh. Eksp. Teor.* **88** 581 (2008)
18. Tokunaga Y et al. *Nature Mater.* **8** 558 (2009)
19. Lobzenko I P, Goncharov P P, Ter-Oganessian N V *J. Phys. Condens. Matter* **27** 246002 (2015)
20. Logginov A S et al. *JETP Lett.* **86** 115 (2007); *Pis'ma Zh. Eksp. Teor. Fiz.* **86** 124 (2007)
21. Arzamastseva G V et al. *JETP* **120** 687 (2015); *Zh. Eksp. Teor. Fiz.* **147** 793 (2015)
22. Zvezdin A K, Pyatakov A P *Phys. Usp.* **52** 845 (2009); *Usp. Fiz. Nauk* **179** 897 (2009)
23. Krichevtsov B B, Pavlov V V, Pisarev R V *JETP Lett.* **49** 535 (1989); *Pis'ma Zh. Eksp. Teor.* **49** 466 (1989)
24. Koronovskyy V E, Ryabchenko S M, Kovalenko V F *Phys. Rev. B* **71** 172402 (2005)
25. Veshchunov I S et al. *Phys. Rev. Lett.* **115** 027601 (2015)
26. Krichevtsov B B, Pisarev R V, Selitskii A G *JETP Lett.* **41** 317 (1985); *Pis'ma Zh. Eksp. Teor.* **41** 259 (1985)
27. Krichevtsov B B, Pisarev R V, Selitskii A G *Sov. Phys. JETP* **74** 565 (1992); *Zh. Eksp. Teor. Fiz.* **101** 1056 (1992)
28. Logginov A S et al. *Appl. Phys. Lett.* **93** 182510 (2008)
29. Logginov A et al. *Solid State Phenomena* **152** 143 (2009)
30. Pyatakov A P et al. *J. Phys. Conf. Ser.* **200** 032059 (2010)
31. Pyatakov A P et al. *Europhys. Lett.* **93** 17001 (2011)
32. Sergeev A S et al. *Izv. Ross. Akad. Nauk Ser. Fiz.* **77** 1523 (2013)
33. Sechin D A, Nikolaeva E P, Pyatakov A P et al. *Solid State Phenomena* **233–234** 443 (2015)
34. Bodunova A S et al., in *Moscow Intern. Symp. on Magnetism, August 21–25, 2011, Book of Abstracts 2011* (Eds N Petrov et al.) (Moscow: Faculty of Physics, Lomonosov Moscow State Univ., 2011) p. 486
35. Geng Y, Wu W *Rev. Sci. Instrum.* **85** 053901 (2014)
36. Mamin R F, Bdikin I K, Kholkin A L *Appl. Phys. Lett.* **94** 222901 (2009)
37. Pyatakov A P et al. *Ferroelectrics* **438** 79 (2012)
38. Balbashov A M, Logginov A S, Shabaeva E P *Sov. Phys. Tech. Phys.* **36** 680 (1991); *Zh. Tekh. Fiz.* **61** (6) 159 (1991);
39. Pyatakov A P "Magnitoelektricheskie i fleksomagnitoelektricheskie effekty v mul'tiferroikakh i magnitnykh dielektrikakh" ("Magnetoelectric and flexomagnetoelectric effects in multiferroics and magnetic dielectrics"), Doctoral Thesis Phys.-Math. Sci. (Moscow: Lomonosov Moscow State Univ., 2013)
40. Pyatakov A et al., in *Intern. Workshop on Phase Transitions and Inhomogeneous States in Oxides, June 22–25, 2015, Kazan, Russia, Book of Abstracts* (Kazan: Kazan Federal Univ., 2015) p. 24
41. Logginov A S et al. *JETP* **90** 499 (2000); *Zh. Eksp. Teor. Fiz.* **117** 571 (2000)
42. Kabychenkov A F, Lisovskii F V, Mansvetova E G *JETP Lett.* **97** 265 (2013); *Pis'ma Zh. Eksp. Teor. Fiz.* **97** 304 (2013)
43. Bar'yakhtar V G, L'vov V A, Yablonskii D A *JETP Lett.* **37** 673 (1983); *Pis'ma Zh. Eksp. Teor. Fiz.* **37** 565 (1983)
44. Khalfina A A, Shamsutdinov M A *Ferroelectrics* **279** 19 (2002)
45. Mostovoy M *Phys. Rev. Lett.* **96** 067601 (2006)
46. Dzyaloshinskii I *Europhys. Lett.* **83** 67001 (2008)
47. Shamsutdinov M A, Kharisov A T, Nikolaev Yu E *Phys. Met. Metallogr.* **111** 451 (2011); *Fiz. Met. Metalloved.* **111** 472 (2011)
48. Sparavigna A, Strigazzi A, Zvezdin A *Phys. Rev. B* **50** 2953 (1994)
49. Balbashov A M, Lisovskii F V, Mansvetova E G, Preprint No. 25(500) (Moscow: Inst. of Radio-Engineering and Electronics, Acad. Sci. USSR, 1988)
50. Malozemoff A P, Slonczewski J C *Magnetic Domain Walls in Bubble Materials* (New York: Academic Press, 1979); Translated into Russian: *Domennye Stenki v Materialakh s Tsilindricheskimi Magnitnymi Domenami* (Moscow: Mir, 1982)
51. Chetkin M V et al. *Sov. Phys. JETP* **67** 2269 (1988); *Zh. Eksp. Teor. Fiz.* **94** (5) 164 (1988)
52. Kandaurova G S, Pamyatnykh L A *Sov. Phys. Solid State* **31** 1351 (1989); *Fiz. Tverd. Tela* **31** (8) 132 (1989)
53. Chetkin M V et al. *JETP Lett.* **49** 204 (1989); *Pis'ma Zh. Eksp. Teor. Fiz.* **49** 174 (1989)
54. Salje E K H, Scott J F *Appl. Phys. Lett.* **105** 252904 (2014)
55. Sergeev A S, PhD Thesis Phys-Math. Sci. (Moscow: Lomonosov Moscow State Univ., 2014)
56. Kim S K, Tchernyshyov O *Phys. Rev. B* **88** 174402 (2013)
57. Andreas C, Kákay A, Hertel R *Phys. Rev. B* **89** 134403 (2014)
58. Bogdanov A N, Yablonskii D A *Sov. Phys. JETP* **68** 101 (1989); *Zh. Eksp. Teor. Fiz.* **95** 178 (1989)
59. Bogdanov A N et al. *Phys. Rev. B* **66** 214410 (2002)
60. Rössler U K, Bogdanov A N, Pfleiderer C *Nature* **442** 797 (2006)

61. Kiselev N S et al. *Phys. Rev. Lett.* **107** 179701 (2011)
62. Mühlbauer S et al. *Science* **323** 915 (2009)
63. Yu X Z et al. *Nature Mater.* **10** 106 (2011)
64. Kiselev N S et al. *J. Phys. D Appl. Phys.* **44** 392001 (2011)
65. Zang J et al. *Phys. Rev. Lett.* **107** 136804 (2011)
66. Schulz T et al. *Nature Phys.* **8** 301 (2012)
67. Seki S et al. *Science* **336** 198 (2012)
68. Murakawa H et al. *Phys. Rev. B* **85** 174106 (2012)
69. Seki S, Ishiwata S, Tokura Y *Phys. Rev. B* **86** 060403(R) (2012)
70. Ruff E et al. *Sci. Rep.* **5** 15025 (2015); arXiv:1504.03918
71. Kézsmárki I et al. *Nature Mater.* **14** 1116 (2015)
72. Ruff E et al. *Sci. Adv.* **1** e1500916 (2015); arXiv:1504.00309
73. Meshkov G A et al. *J. Magn. Soc. Jpn.* **36** (1 – 2) 46 (2012)
74. Zvezdin K A *Phys. Solid State* **42** 120 (2000); *Fiz. Tverd. Tela* **42** 116 (2000)
75. Khvalkovskiy A V et al. *J. Phys. D Appl. Phys.* **46** 074001 (2013)
76. Sizov A D et al. *Uchenye Zapiski Fiz. Fakul't. Mosk. Univ.* (6) 136302 (2013)
77. Popov A I, Plokhov D I, Zvezdin A K *Phys. Rev. B* **90** 214427 (2014)
78. Vakhitov R M, Kharisov A T, Nikolaev Yu E *Dokl. Phys.* **59** 119 (2014); *Dokl. Ross. Akad. Nauk* **455** 150 (2014)
79. Tretiakov O A, Abanov Ar *Phys. Rev. Lett.* **105** 157201 (2010)
80. Thiaville A et al. *Europhys. Lett.* **100** 57002 (2012)
81. Chen H-B, Liu Y-H, Li Y-Q *J. Appl. Phys.* **115** 133913 (2014)
82. Krotenko N B, Melikhov Yu V, Yablonskii D A *Fiz. Tverd. Tela* **27** 3230 (1985)
83. Ekomasov E G *Low Temp. Phys.* **29** 657 (2003); *Fiz. Nizk. Temp.* **29** 878 (2003)
84. Gareeva Z V, Zvezdin A K *Phys. Solid State* **52** 1714 (2010); *Fiz. Tverd. Tela* **52** 1595 (2010)
85. Gareeva Z V, Zvezdin A K *Europhys. Lett.* **91** 47006 (2010)
86. Gareeva Z et al. *Phys. Rev. B* **91** 060404(R) (2015)
87. Pyatakov A P, Meshkov G A, Logginov A S *Moscow Univ. Phys. Bull.* **65** 329 (2010); *Vestn. Moscow Univ. Ser. 3. Fiz. Astron.* (4) 92 (2010)